# Data-driven Voltage Regulation in Radial Power Distribution Systems

Hanchen Xu, Alejandro D. Domínguez-García, *Member, IEEE,* Venugopal V. Veeravalli, *Fellow, IEEE,* and Peter W. Sauer, *Life Fellow, IEEE*

***Abstract*—In this paper, we develop a data-driven framework for controlling distributed energy resources (DERs) in a balanced radial power distribution system with the objective of regulating voltages across the whole system. The objective is to determine optimal DER power injections that minimize the voltage excursions outside a desirable voltage range without knowing a complete model of the power distribution system. To this end, we approximate the nonlinear relationship between the voltage magnitudes and the power injections by a linear model. The parameters of this linear model—referred to as the voltage sensitivities—can be computed using information on the network topology and the line parameters, the values of which will be estimated. Assuming the knowledge of feasible network topology configurations and distribution line resistance-to-reactance ratios, we propose a framework for identifying the true network topology configuration and the corresponding line parameters using only a few measurements of voltage magnitudes and power injections. Utilizing the estimated voltage sensitivities, the optimal DER power injections can be readily determined by solving a convex optimization problem. Due to its data-driven nature, the proposed framework is intrinsically adaptive to changes in system conditions such as unknown topology reconfiguration. The effectiveness of the proposed framework is validated via numerical simulations on the IEEE 123-bus distribution test feeder.**

***Index Terms*—power distribution system, distributed energy resource, voltage regulation, line parameter estimation, topology estimation, data-driven control, sensitivity analysis.**

## NOMENCLATURE

| | |
|---|---|
| *Sets:* | |
| $\mathbb{R}$ | set of real numbers |
| $\mathcal{G}=(\mathcal{N},\mathcal{E})$ | directed graph representing a power distribution system |
| $\mathcal{N}=\{0,1,\cdots,N\}$ | set of buses |
| $\mathcal{N}^g=\{1,\cdots,n\}$ | index set of DERs |
| $\mathcal{E}=\mathcal{N}\times\mathcal{N}$ | set of distribution lines |
| $\mathcal{L}=\{1,\cdots,L\}$ | index set of distribution lines |
| $\mathcal{M}=\{\boldsymbol{M}_1,\cdots,\boldsymbol{M}_\tau\}$ | set of feasible values for $\boldsymbol{M}$ |
| $\mathcal{Z}=\{\boldsymbol{\zeta}_1,\cdots,\boldsymbol{\zeta}_\tau\}$ | set of feasible "$r$-to-$x$" ratio vectors |
| $\mathcal{K}=\{k-m,\cdots,k\}$ | index set of measurements used for estimation |
| *Matrices:* | |
| $\boldsymbol{C}$ | mapping matrix between DER indices and buses |
| $\tilde{\boldsymbol{M}}$ | node-to-edge incidence matrix of $\mathcal{G}$ |
| $\boldsymbol{M}$ | reduced node-to-edge incidence matrix of $\mathcal{G}$ |
| $\boldsymbol{P}$ | path matrix of $\mathcal{G}$ |
| $\boldsymbol{R},\boldsymbol{X}$ | voltage sensitivity matrices |
| $\boldsymbol{W}^p,\boldsymbol{W}^q$ | non-negative diagonal matrices |
| *Vectors:* | |
| $\mathbf{1}$ | all-ones vector |
| $\mathbf{0}$ | all-zeros vector |
| $\boldsymbol{e}$ | basis vector |
| $\boldsymbol{r}=[r_1,\cdots,r_L]^\top$ | line resistance vector |
| $\boldsymbol{x}=[r_1,\cdots,r_L]^\top$ | line reactance vector |
| $\boldsymbol{\zeta}=[\zeta_1,\cdots,\zeta_L]^\top$ | line "$r$-to-$x$" ratio vector |
| $\boldsymbol{p}^g=[p_1^g,\cdots,p_n^g]^\top$ | DER active power injection vector |
| $\boldsymbol{q}^g=[q_1^g,\cdots,q_n^g]^\top$ | DER reactive power injection vector |
| $\boldsymbol{p}^d=[p_1^d,\cdots,p_N^d]^\top$ | active power load vector |
| $\boldsymbol{q}^d=[q_1^d,\cdots,q_N^d]^\top$ | reactive power load vector |
| $\underline{\boldsymbol{p}}^g=[\underline{p}_1^g,\cdots,\underline{p}_n^g]^\top$ | DER minimum active power injection vector |
| $\overline{\boldsymbol{p}}^g=[\overline{p}_1^g,\cdots,\overline{p}_n^g]^\top$ | DER maximum active power injection vector |
| $\underline{\boldsymbol{q}}^g=[\underline{q}_1^g,\cdots,\underline{q}_n^g]^\top$ | DER minimum reactive power injection vector |
| $\overline{\boldsymbol{q}}^g=[\overline{q}_1^g,\cdots,\overline{q}_n^g]^\top$ | DER maximum reactive power injection vector |
| $\boldsymbol{p}=[p_1,\cdots,p_N]^\top$ | net active power injection vector |
| $\boldsymbol{q}=[q_1,\cdots,q_N]^\top$ | net reactive power injection vector |
| $\boldsymbol{V}=[V_1,\cdots,V_N]^\top$ | voltage magnitude vector |
| $\boldsymbol{v}=[v_1,\cdots,v_N]^\top$ | square voltage magnitude vector, where $v_i:=V_i^2$ |
| $\tilde{\boldsymbol{v}}=\boldsymbol{v}-v_0\mathbf{1}_N$ | square voltage magnitude difference vector |
| $\underline{\boldsymbol{v}}=[\underline{V}_1^2,\cdots,\underline{V}_N^2]^\top$ | minimum square voltage magnitude vector |
| $\overline{\boldsymbol{v}}=[\overline{V}_1^2,\cdots,\overline{V}_N^2]^\top$ | maximum square voltage magnitude vector |
| $\boldsymbol{\varepsilon}$ | residual error vector |
| *Scalars:* | |
| $\epsilon$ | residual error |
| $\eta$ | forgetting factor |
| $\beta_1,\beta_2$ | non-negative real numbers |
| *Operators:* | |
| $\mathrm{diag}(\cdot)$ | returns a diagonal matrix with entries of the argument on its diagonal |
| $\|\cdot\|$ | $L_2$ norm |
| $[\cdot]$ | returns the argument if it is positive and zero otherwise |

The authors are with the Department of Electrical and Computer Engineering at the University of Illinois at Urbana-Champaign, Urbana, IL 61801, USA. Email: {hxu45, aledan, vvv, psauer}@illinois.edu.

## I. Introduction

VOLTAGE regulation in power distribution networks is typically accomplished by voltage regulators, load tap changers, and shunt capacitors [1]–[3]. In addition, and also for the purpose of voltage regulation, some recent works have also proposed the use of distributed energy resources (DERs) with fast-responding characteristics [4]–[8]. For example, in [4], the authors proposed a two-stage distributed architecture for voltage regulation in power distribution systems, where in the first stage, a controller located at each node attempts to regulate voltage locally by controlling the reactive power injected at that node, and any deficiency is compensated in the second stage by other DERs providing more reactive power so as to uniformly raise the voltage profile across the system. In [6], by leveraging some relaxation techniques, the authors formulated the voltage regulation problem as a convex optimization problem, the solution of which provides the optimal DER reactive power injection set-points. However, most existing voltage regulation schemes using DERs assume perfect knowledge of the power distribution system model, and thus they may not work properly in the absence of an accurate model. In addition, the power distribution system model may periodically change due to operations such as topology reconfiguration for loss minimization or load balancing [9]. As such, voltage regulation schemes that can adapt to changes in system conditions and are robust against model errors are indeed more desirable in power distribution systems.

In situations where an accurate system model is unavailable, data-driven methods can be applied as an alternative. A key idea in these methods is to approximate the nonlinear relation between the outputs of interest (e.g., voltage magnitudes) and the controls (e.g., power injections) by a linear model, the parameters of which are referred to as the sensitivities (see, e.g., [10]–[16]). These sensitivities are then estimated from the measurements using some regression algorithms such as least-squares regression [10] or ensemble regression [15]. This idea has been pursued in estimation of injection shift factors and power transfer distribution factors [10], and loss factors [12], [13]. The sensitivities have also been utilized in voltage regulation problems [14]–[16]. For example, the authors in [16] proposed a least-squares regression based voltage sensitivity estimation method for unbalanced power distribution systems, where the correlation of measurements taken across time is utilized. In [14], the authors proposed ambient signal based estimation methods for volt-to-var sensitivities in transmission systems. In [15], they further developed data-driven sequential voltage control methods based on estimated volt-to-var sensitivities and demonstrated the effectiveness via simulations using realistic data. Utilizing the voltage sensitivities, the nonlinear relation between the voltage magnitudes and the power injections are substituted with a linear relation, based on which the voltage regulation problem using DERs can be cast as a convex optimization problem that can be solved easily.

The sensitivities estimated from measurements can have several nice properties, including adaptivity to changes in system conditions such as topology reconfigurations or parameter changes. However, existing approaches directly estimate all elements of the sensitivities; consequently, the resulting regression problem usually has a large number of unknowns. In order to obtain accurate estimates of the sensitivities, a significant amount of measurements are required. Moreover, these measurements need to be taken at a high sampling rate so as to quickly track changes in system operating conditions. This may be feasible in transmission systems equipped with phasor measurement units, but it may be impractical for power distribution systems. Therefore, methods that can efficiently estimate the sensitivities without requiring a large amount of measurements are yet to be developed.

In this paper, we focus on the problem of controlling DERs for voltage regulation in a balanced radial power distribution system, relying only on an incomplete distribution system model. We will pursue the idea of data-driven methods and utilize estimated voltage sensitivities to determine the power injections from DERs. The key challenge that needs to be tackle here is how to efficiently estimate the voltage sensitivities from a few measurements that are taken from the power distribution system. To this end, we fully exploit the structural characteristics of balanced radial power distribution systems to significantly reduce the number of parameters to be estimated, and consequently reducing the number of measurements required. Specifically, for balanced radial power distribution systems, the nonlinear relationships between voltage magnitudes and power injections can be approximated by a linear model—the so-called LinDistFlow model [9], which has been widely used in voltage control problems of balanced radial power distribution systems (see, e.g., [8], [17], [18]). The coefficients of the LinDistFlow model are essentially the sensitivities of the squared voltage magnitudes with respect to active and reactive power injections, i.e., the voltage sensitivities, and can be computed directly using system topology and line parameter information. Assuming the knowledge of feasible topology configurations and distribution line resistance-to-reactance ("$r$-to-$x$") ratios, which are typically available and do not change during a relatively short time period, the estimation of the voltage sensitivities can be reduced to the estimation of the true topology configuration and corresponding line parameters, which can be effectively accomplished using a few voltage magnitude and power injection measurements. Using the estimated voltage sensitivities, the optimal DER power injections can be readily determined by solving an easily solvable convex optimization problem. Our theoretical analysis shows that the voltage sensitivities of interest are easily identifiable.

This paper has extended our earlier results in [19] in several directions, and our major contributions include the following:

1) the development of a efficient voltage sensitivity estimation algorithm that identifies the underlying system topology and respective line parameters;
2) a theoretical analysis regarding the identifiability of the line parameters;
3) extensive numerical simulations on a large distribution test feeder to validate the robustness and effectiveness of the proposed framework.

The remainder of the paper is organized as follows. The power distribution system model adopted in this work and the

voltage regulation problem are introduced in Section II. The details of the proposed voltage regulation framework, including the voltage sensitivity estimator and the voltage controller, are presented in Section III. The identifiability of the voltage sensitivities is analyzed in Section IV. The effectiveness of the proposed framework is validated in Section V through numerical simulations. Some concluding remarks are provided in Section VI.

## II. Preliminaries

In this section, we provide the power distribution system model adopted in this work. Subsequently, we describe the voltage regulation problem.

### A. Power Distribution System Model

Consider a three-phase balanced power distribution system represented by a directed graph $\mathcal{G} = (\mathcal{N}, \mathcal{E})$, where $\mathcal{N} = \{0, 1, \cdots, N\}$ is the set of buses (nodes), and $\mathcal{E} = \mathcal{N} \times \mathcal{N}$ is set of distribution lines (edges). Let $\mathcal{L} = \{1, 2, \cdots, L\}$ be the set indexing the distribution lines. Each distribution line $\ell \in \mathcal{L}$ is associated with $(i, j) \in \mathcal{E}$, where $i$ corresponds to the sending end and $j$ corresponds to the receiving end of line $\ell$, with the direction from $i$ to $j$ defined to be positive. Let $r_\ell$ and $x_\ell$ denote the resistance and reactance of line $\ell \in \mathcal{L}$, respectively, and define $\boldsymbol{r} = [r_1, \cdots, r_L]^\top$ and $\boldsymbol{x} = [x_1, \cdots, x_L]^\top$. Let $\zeta_\ell$ denote the "$r$-to-$x$" ratio of line $\ell$, i.e., $r_\ell / x_\ell = \zeta_\ell$, and define $\boldsymbol{\zeta} = [\zeta_1, \cdots, \zeta_L]^\top$. Throughout the rest of the paper, we make the following assumptions:

**A1**. Bus 0 corresponds to the substation bus that remains a constant voltage magnitude and has no DER or load connected to it.

**A2**. The power distribution system is radial.

**A3**. The "$r$-to-$x$" ratios of all distribution lines are known.

Let $\mathcal{N}^g = \{1, \cdots, n\}$ denote the index set of DERs. In addition, let $p_i^g$ and $q_i^g$ respectively denote the active and reactive power injected by DER $i$, and define $\boldsymbol{p}^g = [p_1^g, \cdots, p_n^g]^\top$ and $\boldsymbol{q}^g = [q_1^g, \cdots, q_n^g]^\top$. Throughout this paper, DERs are modeled as "PQ" buses. Similarly, let $p_i^d$ and $q_i^d$ respectively denote the active and reactive power demand at bus $i$, and define $\boldsymbol{p}^d = [p_1^d, \cdots, p_N^d]^\top$, and $\boldsymbol{q}^d = [q_1^d, \cdots, q_N^d]^\top$. Let $\underline{p}_i^g$ and $\overline{p}_i^g$ respectively denote the minimum and maximum active power that can be provided by DER $i$, and define $\underline{\boldsymbol{p}}^g = [\underline{p}_1^g, \cdots, \underline{p}_n^g]^\top$ and $\overline{\boldsymbol{p}}^g = [\overline{p}_1^g, \cdots, \overline{p}_n^g]^\top$. Similarly, let $\underline{q}_i^g$ and $\overline{q}_i^g$ respectively denote the minimum and maximum reactive power that can be provided by DER $i$, and define $\underline{\boldsymbol{q}}^g = [\underline{q}_1^g, \cdots, \underline{q}_n^g]^\top$ and $\overline{\boldsymbol{q}}^g = [\overline{q}_1^g, \cdots, \overline{q}_n^g]^\top$. Let $\boldsymbol{C} \in \mathbb{R}^{N \times n}$ denote the mapping matrix between the DER indices and the buses, which is defined as follows: the entry at the $i^{\text{th}}$ row, $j^{\text{th}}$ column of $\boldsymbol{C}$ is 1 if DER $j$ is connected to bus $i$ and 0 otherwise. Define $\boldsymbol{p} = [p_1, \cdots, p_N]^\top = \boldsymbol{C}\boldsymbol{p}^g - \boldsymbol{p}^d$, and $\boldsymbol{q} = [q_1, \cdots, q_N]^\top = \boldsymbol{C}\boldsymbol{q}^g - \boldsymbol{q}^d$.

Let $\tilde{\boldsymbol{M}} = [M_{i\ell}] \in \mathbb{R}^{(N+1) \times L}$ denote the node-to-edge incidence matrix of $\mathcal{G}$, which is defined as follows: $M_{i\ell} = 1$ if line $\ell$ starts at bus $i$, $M_{i\ell} = -1$ if line $\ell$ ends at bus $i$, and $M_{i\ell} = 0$ otherwise. Let $\boldsymbol{M}$ denote the $(N \times L)$-dimensional matrix that results from removing the first row of $\tilde{\boldsymbol{M}}$. Under Assumption **A2**, $L = N$, and $\boldsymbol{M}$ is invertible. Note that the topology of the power distribution system is uniquely determined by $\boldsymbol{M}$; therefore, we also refer to $\boldsymbol{M}$ as the system topology configuration. A power distribution system may be operated under various feasible topology configurations. Let $\mathcal{M} = \{\boldsymbol{M}_1, \cdots, \boldsymbol{M}_\tau\}$ denote the set of $\tau$ feasible topology configurations of the power distribution system. Note that each topology configuration is associated with a vector of "$r$-to-$x$" ratios. Let $\mathcal{Z} = \{\boldsymbol{\zeta}_1, \cdots, \boldsymbol{\zeta}_\tau\}$ denote the set of $\tau$ "$r$-to-$x$" ratio vectors associated with $\mathcal{M}$.

Let $V_i$ denote the magnitude of the voltage at bus $i \in \mathcal{N}$; define $\boldsymbol{V} = [V_1, \cdots, V_N]^\top$. Define $v_i := V_i^2$, $\boldsymbol{v} = [v_1, \cdots, v_N]^\top$, and $\tilde{\boldsymbol{v}} = \boldsymbol{v} - v_0 \mathbf{1}_N$; $v_0$ is a constant under Assumption **A1**. Under Assumption **A2**, the relation between $\boldsymbol{v}$, $\boldsymbol{p}$, and $\boldsymbol{q}$, can be approximately captured by the so-called LinDistFlow model as follows (see, e.g., [9]):

$$\tilde{\boldsymbol{v}} = \boldsymbol{R}\boldsymbol{p} + \boldsymbol{X}\boldsymbol{q}, \tag{1}$$

where $\mathbf{1}_N$ is the $N$-dimensional all-ones vector, and

$$\boldsymbol{R} = 2(\boldsymbol{M}^{-1})^\top \mathrm{diag}(\boldsymbol{r}) \boldsymbol{M}^{-1}, \tag{2}$$

$$\boldsymbol{X} = 2(\boldsymbol{M}^{-1})^\top \mathrm{diag}(\boldsymbol{x}) \boldsymbol{M}^{-1}, \tag{3}$$

where $\mathrm{diag}(\cdot)$ returns a diagonal matrix with the entries of the argument on its diagonal. We refer to the matrices $\boldsymbol{R}$ and $\boldsymbol{X}$ as the voltage sensitivity matrices, or simply voltage sensitivities.

### B. Voltage Regulation Problem

The objective here is to maintain the voltage magnitude at each bus $i$, $i \in \mathcal{N}$, of the power distribution system within a pre-specified interval $[\underline{V}_i, \overline{V}_i], 0 \le \underline{V}_i \le \overline{V}_i$. Voltage regulation in power distribution systems can be effectively accomplished by a two-timescale architecture (see, e.g., [7]), where on the slow timescale, slower actuation devices including load tap changers and capacitor banks are adjusted to minimize voltage deviations from the desired range, and on the fast timescale, fast actuators such as DERs are dispatched. In this paper, we focus solely on the latter mechanism for achieving voltage regulation on the fast timescale. Then, the problem is to determine DER active and reactive power injections so that

**[C1.]** the active and reactive power injections from each DER $i$, $i \in \mathcal{N}^g$, do not exceed its corresponding capacity limits, i.e., $\underline{\boldsymbol{p}}^g \le \boldsymbol{p}^g \le \overline{\boldsymbol{p}}^g$, $\underline{\boldsymbol{q}}^g \le \boldsymbol{q}^g \le \overline{\boldsymbol{q}}^g$; and

**[C2.]** the voltage magnitude at each bus $i$, $i \in \mathcal{N}$, is within the pre-specified interval, i.e., $\underline{V}_i \le V_i \le \overline{V}_i$.

In addition, among all feasible values of $\boldsymbol{p}^g$ and $\boldsymbol{q}^g$, we would like to select the ones that minimize some cost function, which reflects the cost of voltage deviations as well as the cost of active and reactive power provision.

Except for $\mathcal{M}$ and $\mathcal{Z}$, which we assume are known, we assume no prior information on the voltage sensitivity matrices. The voltage regulation problem cannot be solved without knowing the voltage sensitivity matrices. Therefore, we will resort to a data-driven approach to estimate voltage sensitivity matrices from measurements of voltage magnitudes and power injections.

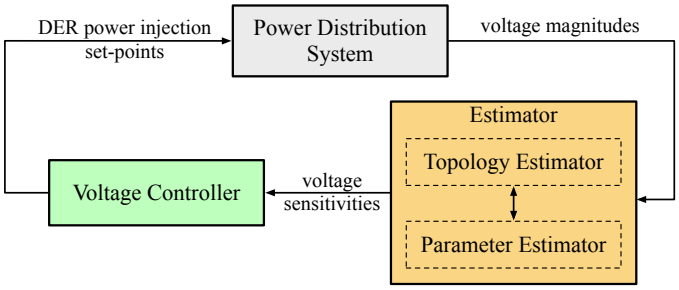


Fig. 1. Data-driven voltage regulation framework.

## III. Voltage Regulation Framework

In this section, we propose an adaptive data-driven framework for voltage regulation using DERs. We first give an overview of the framework and then present the details of its fundamental building blocks.

### A. Framework Overview

The proposed voltage regulation framework consists of two components: a voltage sensitivity estimator and a voltage controller. The interaction between the different components and the power distribution system is illustrated via the block diagram in Fig. 1. The estimator component contains a topology estimator that determines the topology configuration of the power distribution system, i.e., it determines $\boldsymbol{M}$, and a parameter estimator that estimates the line parameters $\boldsymbol{r}$ and $\boldsymbol{x}$ using measurements of power injections and voltage magnitudes. The estimates of the voltage sensitivity matrices $\boldsymbol{R}$ and $\boldsymbol{X}$, denoted respectively by $\hat{\boldsymbol{R}}$ and $\hat{\boldsymbol{X}}$, are computed from estimates of $\boldsymbol{M}$, $\boldsymbol{r}$, and $\boldsymbol{x}$. After that, $\hat{\boldsymbol{R}}$ and $\hat{\boldsymbol{X}}$ are sent to the voltage controller. The voltage controller then computes the set-points for the DER active and reactive power injections that minimize some cost function subject to constraints **C1** and **C2**. The DERs will be instructed to inject the amount of active and reactive power determined by the voltage controller. A new set of measurements will be available once the DERs have modified their power injections. These measurements will be used by the estimator to update $\hat{\boldsymbol{R}}$ and $\hat{\boldsymbol{X}}$ so as to reflect any changes in them. The detailed formulations for the voltage sensitivity problem and the voltage regulation problem are presented next.

### B. Voltage Sensitivity Estimator

At time instant $k+1$, assume we have measurements $V_0[t]$, $\boldsymbol{V}[t]$, $\boldsymbol{p}[t]$, $\boldsymbol{q}[t]$, $t = 0, 1, \cdots, k$, where the index $t$ indicates that the corresponding measurement is obtained at time instant $t$. To reduce the computational burden, we select a subset of measurements, indexed by elements in $\mathcal{K} = \{k-m, \cdots, k\}$. The voltage sensitivities can be estimated based on the LinDistFlow model in (1). The goal of the voltage sensitivity estimator at time instant $k$ is to estimate the values of $\boldsymbol{R}$ and $\boldsymbol{X}$ from the measurements obtained at the time instants in $\mathcal{K}$. We propose a voltage sensitivity estimator that consists of two components, a parameter estimator and a topology estimator. The former aims to estimate the line parameters, given the topology configuration, i.e., $\boldsymbol{M}$, while the latter aims to determine $\boldsymbol{M}$ from $\mathcal{M}$, based on the results from the parameter estimator.

*1) Parameter estimator:* For a given $\boldsymbol{M} \in \mathcal{M}$, estimating $\boldsymbol{R}$ and $\boldsymbol{X}$ boils down to estimating $\boldsymbol{r}$ and $\boldsymbol{x}$. Let $\hat{\boldsymbol{r}}$ and $\hat{\boldsymbol{x}}$ denote the estimates of $\boldsymbol{r}$ and $\boldsymbol{x}$, respectively. We can then formulate the parameter estimation problem by using the relation in (1) as

$$(\hat{\boldsymbol{r}}, \hat{\boldsymbol{x}}) = \underset{(\boldsymbol{r},\boldsymbol{x})}{\arg\min} \sum_{t\in\mathcal{K}} \eta^{k-t} \|\boldsymbol{R}\boldsymbol{p}[t] + \boldsymbol{X}\boldsymbol{q}[t] - \tilde{\boldsymbol{v}}[t]\|^2, \quad (4)$$

subject to

$$\boldsymbol{R} = 2(\boldsymbol{M}^{-1})^\top \mathrm{diag}(\boldsymbol{r})\boldsymbol{M}^{-1}, \quad (5a)$$

$$\boldsymbol{X} = 2(\boldsymbol{M}^{-1})^\top \mathrm{diag}(\boldsymbol{x})\boldsymbol{M}^{-1}, \quad (5b)$$

where $\|\cdot\|$ denotes the $L_2$-norm, $\eta \in (0, 1]$ is a forgetting factor. Essentially, the objective of the parameter estimator is to find the line parameters that fit the LinDistFlow model best for a given topology configuration.

We next show that (5) has a closed-form solution. First note that the matrix $\mathrm{diag}(\boldsymbol{x})$ can be decomposed as follows:

$$\mathrm{diag}(\boldsymbol{x}) = \sum_{\ell=1}^{L} x_\ell \boldsymbol{e}_\ell \boldsymbol{e}_\ell^\top, \quad (6)$$

where $\boldsymbol{e}_\ell$ is the $\ell^{\text{th}}$ basis vector in $\mathbb{R}^L$, i.e., all entries in $\boldsymbol{e}_\ell$ are 0 except the $\ell^{\text{th}}$ entry, which equals to 1. Using (6), we obtain that

$$\begin{aligned}\boldsymbol{X}\boldsymbol{q}[t] &= 2(\boldsymbol{M}^{-1})^\top \mathrm{diag}(\boldsymbol{x})\boldsymbol{M}^{-1}\boldsymbol{q}[t] \\ &= 2(\boldsymbol{M}^{-1})^\top \sum_{\ell=1}^{L} x_\ell \boldsymbol{e}_\ell \boldsymbol{e}_\ell^\top \boldsymbol{M}^{-1}\boldsymbol{q}[t] \\ &= \sum_{\ell=1}^{L} \boldsymbol{\Gamma}_\ell \boldsymbol{q}[t] x_\ell, \end{aligned} \quad (7)$$

where $\boldsymbol{\Gamma}_\ell = 2(\boldsymbol{M}^{-1})^\top \boldsymbol{e}_\ell \boldsymbol{e}_\ell^\top \boldsymbol{M}^{-1}$. Similarly,

$$\begin{aligned}\boldsymbol{R}\boldsymbol{p}[t] &= \sum_{\ell=1}^{L} \boldsymbol{\Gamma}_\ell \boldsymbol{p}[t] r_\ell \\ &= \sum_{\ell=1}^{L} \boldsymbol{\Gamma}_\ell \zeta_\ell \boldsymbol{p}[t] x_\ell. \end{aligned} \quad (8)$$

Let $\boldsymbol{\rho}_\ell[t] = \eta^{\frac{k-t}{2}}(\zeta_\ell \boldsymbol{p}[t] + \boldsymbol{q}[t])$, $\ell \in \mathcal{L}$, and define

$$\boldsymbol{\Psi}[k] = \begin{bmatrix} \boldsymbol{\Gamma}_1\boldsymbol{\rho}_1[k-m] & \cdots & \boldsymbol{\Gamma}_L\boldsymbol{\rho}_L[k-m] \\ \vdots & \vdots & \vdots \\ \boldsymbol{\Gamma}_1\boldsymbol{\rho}_1[k] & \cdots & \boldsymbol{\Gamma}_L\boldsymbol{\rho}_L[k] \end{bmatrix}, \quad (9)$$

and

$$\boldsymbol{\psi}[k] = [\eta^{\frac{m}{2}}\tilde{\boldsymbol{v}}[k-m]^\top, \cdots, \eta^{\frac{0}{2}}\tilde{\boldsymbol{v}}[k]^\top]^\top. \quad (10)$$

Note that $\boldsymbol{\Psi}[k] \in \mathbb{R}^{(m+1)N\times L}$ and $\boldsymbol{\psi}[k] \in \mathbb{R}^{(m+1)N}$ are dependent on $\mathcal{K}$. Then (5) can be equivalently formulated in the classical form of a linear regression problem as follows:

$$\underset{\boldsymbol{x}}{\text{minimize}} \|\boldsymbol{\Psi}[k]\boldsymbol{x} - \boldsymbol{\psi}[k]\|^2, \quad (11)$$

the solution to which is given by

$$\hat{\boldsymbol{x}} = \boldsymbol{\Psi}[k]^{\dagger}\boldsymbol{\psi}[k] \tag{12}$$

where $\boldsymbol{\Psi}[k]^{\dagger} = (\boldsymbol{\Psi}[k]^{\top}\boldsymbol{\Psi}[k])^{-1}\boldsymbol{\Psi}[k]^{\top}$ denotes the pseudo-inverse of $\boldsymbol{\Psi}[k]$. When $\boldsymbol{\Psi}[k]^{\top}\boldsymbol{\Psi}[k]$ is singular, $\boldsymbol{\Psi}[k]^{\dagger}$ can be obtained via singular value decomposition (SVD). Note that $\boldsymbol{\Psi}[k]$ needs to have full rank, i.e., $\mathrm{rank}(\boldsymbol{\Psi}[k]) = L$, in order to be able to estimate $\boldsymbol{x}$. The resistance vector is estimated as

$$\hat{\boldsymbol{r}} = \mathrm{diag}(\boldsymbol{\zeta})\hat{\boldsymbol{x}}. \tag{13}$$

*Remark* 1. The parameter estimator proposed here requires the availability of measurements of active and reactive power injections, as well as voltage magnitudes at all buses. In the case where such measurements at some buses are unavailable at all time, the LinDistFlow model in (1) cannot be directly utilized to solve for the line parameters. The development of an efficient parameter estimator under partial system observability requires further investigation and we leave it for future work.

*2) Topology estimator:* Define a residual vector, denoted by $\boldsymbol{\varepsilon}$, as follows:

$$\boldsymbol{\varepsilon} = \hat{\boldsymbol{R}}\boldsymbol{p} + \hat{\boldsymbol{X}}\boldsymbol{q} - \tilde{\boldsymbol{v}}, \tag{14}$$

where

$$\hat{\boldsymbol{R}} = 2(\boldsymbol{M}^{-1})^{\top}\mathrm{diag}(\hat{\boldsymbol{r}})\boldsymbol{M}^{-1}, \tag{15}$$

$$\hat{\boldsymbol{X}} = 2(\boldsymbol{M}^{-1})^{\top}\mathrm{diag}(\hat{\boldsymbol{x}})\boldsymbol{M}^{-1}. \tag{16}$$

Given a set of measurements, we can compute a residual vector for each $\boldsymbol{M} \in \mathcal{M}$.

The objective of the topology estimator is to find $\boldsymbol{M} \in \mathcal{M}$ such that a weighted sum of $\|\boldsymbol{\varepsilon}\|$ over several time instants is minimized. At time instant $k+1$, the topology estimation problem can be formulated as:

$$\hat{\boldsymbol{M}} = \underset{\boldsymbol{M}\in\mathcal{M}}{\arg\min}\, \epsilon_{\boldsymbol{M}}, \tag{17}$$

with

$$\epsilon_{\boldsymbol{M}} = \sum_{t\in\mathcal{K}} \eta^{k-t}\|\boldsymbol{\varepsilon}[t]\|, \tag{18}$$

where $\boldsymbol{\varepsilon}[t]$ is computed through (14) to (16). We refer to $\epsilon_{\boldsymbol{M}}$ as the *residual error* associated with topology configuration $\boldsymbol{M}$. Essentially, the topology estimator selects the topology under which the residual error $\epsilon_{\boldsymbol{M}}$ is minimized, where the line parameters are estimated by the parameter estimator. The intuition here is that different topology configurations will impose different structural constraints on voltage sensitivity matrices, which consequently impacts the residual error. The true topology configuration is expected to result in the least residual error.

The voltage sensitivity estimation algorithm is summarized in Algorithm 1. Note that the residual error and the line parameters corresponding to each topology configuration can be computed in parallel. In practice, the number of switches in typical distribution systems is not large, so is the number of feasible topology configurations that satisfy Assumption **A2**. Therefore, the scalability of Algorithm 1 is mainly determined by the line parameter estimator that solves a least-squares regression problem of $L$ unknowns as shown in (11).

**Algorithm 1:** Voltage Sensitivity Estimation

**Input:**

$\mathcal{M}$: set of feasible topology configurations

$\mathcal{Z}$: set of "$r$-to-$x$" ratio vectors

$\boldsymbol{p}[t], \boldsymbol{q}[t], \boldsymbol{v}[t]$: active power, reactive power, voltage magnitude measurements, $t \in \mathcal{K}$

**Output:**

$\hat{\boldsymbol{M}}$: estimated topology configuration

$\hat{\boldsymbol{r}}, \hat{\boldsymbol{x}}$: estimated line parameters

**for** $\boldsymbol{M} \in \mathcal{M}$, $\boldsymbol{\zeta} \in \mathcal{Z}$ **do**

Construct $\boldsymbol{\Psi}$ and $\boldsymbol{\psi}$ according to (9) and (10)

Compute pseudo-inverse of $\boldsymbol{\Psi}$, i.e., $\boldsymbol{\Psi}^{\dagger}$

Compute line parameters using

$$\hat{\boldsymbol{x}} = \boldsymbol{\Psi}^{\dagger}\boldsymbol{\psi}, \hat{\boldsymbol{r}} = \mathrm{diag}(\boldsymbol{\zeta})\hat{\boldsymbol{x}}$$

Compute voltage sensitivities using

$$\hat{\boldsymbol{R}} = 2(\boldsymbol{M}^{-1})^{\top}\mathrm{diag}(\hat{\boldsymbol{r}})\boldsymbol{M}^{-1}$$
$$\hat{\boldsymbol{X}} = 2(\boldsymbol{M}^{-1})^{\top}\mathrm{diag}(\hat{\boldsymbol{x}})\boldsymbol{M}^{-1}$$

Compute the residual error via

$$\epsilon_{\boldsymbol{M}} = \sum_{t\in\mathcal{K}} \eta^{k-t}\|\hat{\boldsymbol{R}}\boldsymbol{p}[t] + \hat{\boldsymbol{X}}\boldsymbol{q}[t] - \tilde{\boldsymbol{v}}[t]\|^2$$

**end**

Select topology configuration $\hat{\boldsymbol{M}}$ using

$$\hat{\boldsymbol{M}} = \underset{\boldsymbol{M}\in\mathcal{M}}{\arg\min}\, \epsilon_{\boldsymbol{M}}$$

and line parameters $\hat{\boldsymbol{r}}, \hat{\boldsymbol{x}}$ to be the ones associated with $\hat{\boldsymbol{M}}$

### C. Voltage Controller

The voltage controller aims to determine the set-points for the DER active and reactive power injections while meeting all requirements discussed in Section II-B. Note that for a given set of power injections, the resulting voltage magnitude at each bus can be estimated using (1), where $\hat{\boldsymbol{R}}$ and $\hat{\boldsymbol{X}}$ are used instead of $\boldsymbol{R}$ and $\boldsymbol{X}$. Define $\underline{\boldsymbol{v}} = [\underline{V}_1^2, \cdots, \underline{V}_N^2]^{\top}$ and $\overline{\boldsymbol{v}} = [\overline{V}_1^2, \cdots, \overline{V}_N^2]^{\top}$. Then, the voltage control problem can be formulated as the following convex optimization problem:

$$\underset{\boldsymbol{p}^g, \boldsymbol{q}^g}{\text{minimize}}\ \ c(\boldsymbol{p}^g, \boldsymbol{q}^g), \tag{19}$$

subject to

$$\boldsymbol{v} = \hat{\boldsymbol{R}}(\boldsymbol{C}\boldsymbol{p}^g - \boldsymbol{p}^d) + \hat{\boldsymbol{X}}(\boldsymbol{C}\boldsymbol{q}^g - \boldsymbol{q}^d) + v_0\mathbf{1}_N, \tag{20a}$$

$$\underline{\boldsymbol{p}}^g \le \boldsymbol{p}^g \le \overline{\boldsymbol{p}}^g, \underline{\boldsymbol{q}}^g \le \boldsymbol{q}^g \le \overline{\boldsymbol{q}}^g, \tag{20b}$$

with

$$\begin{aligned} c(\boldsymbol{q}^g) =& (\boldsymbol{p}^g)^{\top}\boldsymbol{W}^p\boldsymbol{p}^g + (\boldsymbol{q}^g)^{\top}\boldsymbol{W}^q\boldsymbol{q}^g \\ &+ \beta_1\|[\underline{\boldsymbol{v}} - \boldsymbol{v}]_+\|^2 + \beta_2\|[\boldsymbol{v} - \overline{\boldsymbol{v}}]_+\|^2, \end{aligned} \tag{21}$$

where $\boldsymbol{W}^p = \mathrm{diag}(w_1^p, \cdots, w_n^p)$, $\boldsymbol{W}^q = \mathrm{diag}(w_1^q, \cdots, w_n^q)$ are non-negative diagonal matrices, $[\cdot]_+$ returns its argument if the argument is positive and zero otherwise, and $\beta_1$ and $\beta_2$ are non-negative weights. The first two terms of $c(\cdot)$ are costs associated with the active and reactive power injections,

respectively, while the last two terms penalize the violation of constraint **C2**.

Constraint (20a) is the LinDistFlow model, which is used to estimate the voltage magnitudes for given power injections. Note that $\boldsymbol{p}^d$ and $\boldsymbol{q}^d$ are measured before solving the voltage control problem. The optimization problem in (19)-(21) is a simple convex optimization problem that can be easily solved using existing solvers such as Gurobi [20]. Solving the voltage control problem gives the optimal set-points for the DER active and reactive power injections.

Note that more complex constraints such as constraints on power factors and line power flows can be readily incorporated into the formulation of the voltage control problem. Yet, the formulation of the voltage control problem is not a contribution of ours; thus, we will focus on the most fundamental formulation throughout this paper.

## IV. Voltage Sensitivity Identifiability

In this section, we first introduce the path matrix and then analyze the conditions under which the line parameters and correspondingly voltage sensitivities, can be identified.

### A. Path Matrix

Let $\mathcal{P}_i \subseteq \mathcal{L}$ denote the set of lines that form a path from bus 0—referred to as the root—to bus $i$. Since the power distribution system is radial, then $\mathcal{P}_i$ is unique (see Theorem 2.1.4 in [21]). Bus $i$ is a leaf if for all $j \in \mathcal{N} \setminus \{i\}$, $(i,j) \notin \mathcal{E}$, i.e., there are no distribution lines starting at bus $i$. We say bus $i$ is closer to the root than bus $j$ if $|\mathcal{P}_i| < |\mathcal{P}_j|$, where $|\cdot|$ denotes the cardinality of a set. In defining $\boldsymbol{M}$, we choose the sending end of a line to be the bus that is closer to the root. Let $\boldsymbol{P} = [P_{\ell i}] \in \mathbb{R}^{L\times N}$ denote the path matrix of $\mathcal{G}$, with $P_{\ell i} = 1$ if line $\ell$ is on $\mathcal{P}_i$, and all other entries equal to zero. Under this setup, the relation between $\boldsymbol{P}$ and $\boldsymbol{M}$ is given by the following lemma.

**Lemma 1.** $\boldsymbol{P}$ and $\boldsymbol{M}$ are related as follows: $\boldsymbol{M}^{-1} = -\boldsymbol{P}$.

*Proof.* (See also Theorem 2.10 in [22].) Consider the entry at the $i^{\text{th}}$ row and $j^{\text{th}}$ column in $\boldsymbol{MP}$, which is $\sum_{\ell=1}^{L} M_{i\ell}P_{\ell j}$.

1) Consider first the case when $i = j$. If line $\ell$ is not connected to bus $i$, then $M_{i\ell} = 0$. If line $\ell$ starts at bus $i$, then $M_{i\ell} = 1$ and $P_{\ell i} = 0$ (because line $\ell$ is not on $\mathcal{P}_i$—the path from the root to bus $i$). If line $\ell$ ends at bus $i$, then $M_{i\ell} = -1$ and $P_{\ell i} = 1$. Obviously, there is one line that ends at bus $i$. Moreover, such a line is unique since otherwise there would be two paths from the root to bus $i$. Therefore, $\sum_{\ell=1}^{L} M_{i\ell}P_{\ell i} = M_{i\ell_i}P_{\ell_i i} = -1$, where line $\ell_i \in \mathcal{L}$ is the line that ends at $i$.
2) Next consider the case where $i \neq j$. Similar to the previous case, we only need to consider the lines that start from or end at bus $i$.
   a) If line $\ell$ ends at bus $i$, then $M_{i\ell} = -1$. If $\ell \notin \mathcal{P}_j$, then $P_{\ell j} = 0$ and $M_{i\ell}P_{\ell j} = 0$. If $\ell \in \mathcal{P}_j$, then $P_{\ell j} = 1$. In the latter case, there must exist a unique line $\ell' \in \mathcal{P}_j$ that starts at $i$. Then $M_{i\ell}P_{\ell j} + M_{i\ell'}P_{\ell' j} = -1+1 = 0$. Therefore, $\sum_{\ell=1}^{L} M_{i\ell}P_{\ell j} = 0$.
   b) If line $\ell$ starts at bus $i$, then $M_{i\ell} = 1$. If $\ell \notin \mathcal{P}_j$, then $P_{\ell j} = 0$ and $M_{i\ell}P_{\ell j} = 0$. If $\ell \in \mathcal{P}_j$, then $P_{\ell j} = 1$. In the latter case, there must exist a unique line $\ell' \in \mathcal{P}_j$ that ends at $i$. Similar to the previous argument, $\sum_{\ell=1}^{L} M_{i\ell}P_{\ell j} = 0$.

To summarize, $\sum_{\ell=1}^{L} M_{i\ell}P_{\ell j}$ equals to 1 if $i = j$ and 0 otherwise; therefore, $\boldsymbol{M}^{-1} = -\boldsymbol{P}$. □

The path matrix plays an important role in the identifiability analysis of the voltage sensitivities to be detailed next.

### B. Identifiability Analysis

Before presenting the result on the identifiability of voltage sensitivities, we introduce the concept of downstream buses.

**Definition 1.** If line $\ell \in \mathcal{P}_i$, $\ell \in \mathcal{L}$, i.e., line $\ell$ is on the path from the root to bus $i$, then bus $i$ is a downstream bus of line $\ell$. The set of downstream buses of line $\ell$ is denoted by $\mathcal{N}_\ell$.

As discussed in Section III-B, $\boldsymbol{\Psi}[k]$ needs to have full rank, i.e., $\text{rank}(\boldsymbol{\Psi}[k]) = L$, in order to be able to estimate $\boldsymbol{x}$ by using (12). When $\boldsymbol{\Psi}$ does not have a full rank, some of the line parameters cannot be estimated from the measurements. The main results for the voltage sensitivity identifiability is stated as follows:

**Theorem 1.** The parameters of line $\ell \in \mathcal{L}$ are identifiable if and only if the following condition is satisfied for some $t \in \mathcal{K}$:

$$\sum_{i\in\mathcal{N}_\ell} \zeta_\ell p_i[t] + q_i[t] \neq 0. \tag{22}$$

*Proof.* Using the path matrix, $\boldsymbol{\Gamma}_\ell$ can be written as $\boldsymbol{\Gamma}_\ell = 2\boldsymbol{P}^\top \boldsymbol{e}_\ell \boldsymbol{e}_\ell^\top \boldsymbol{P}$. Note that $\boldsymbol{P}^\top \boldsymbol{e}_\ell$ is the $\ell^{\text{th}}$ column of $\boldsymbol{P}^\top$ and $\boldsymbol{\Gamma}_\ell$ is a rank-one matrix. Let $\boldsymbol{\pi}_\ell = \boldsymbol{P}^\top \boldsymbol{e}_\ell$, then $\boldsymbol{P}^\top = [\boldsymbol{\pi}_1, \cdots, \boldsymbol{\pi}_L]$. Thus,

$$\boldsymbol{\Gamma}_\ell = 2\boldsymbol{P}^\top \boldsymbol{e}_\ell \boldsymbol{e}_\ell^\top \boldsymbol{P} = 2\boldsymbol{\pi}_\ell \boldsymbol{\pi}_\ell^\top, \tag{23}$$

and $\boldsymbol{\Psi}[k]$ can be written as

$$\boldsymbol{\Psi}[k] = 2\begin{bmatrix} \boldsymbol{\pi}_1\boldsymbol{\pi}_1^\top \boldsymbol{\rho}_1[k-m] & \cdots & \boldsymbol{\pi}_L\boldsymbol{\pi}_L^\top \boldsymbol{\rho}_L[k-m] \\ \vdots & \vdots & \vdots \\ \boldsymbol{\pi}_1\boldsymbol{\pi}_1^\top \boldsymbol{\rho}_1[k] & \cdots & \boldsymbol{\pi}_L\boldsymbol{\pi}_L^\top \boldsymbol{\rho}_L[k] \end{bmatrix}. \tag{24}$$

Let $\mathcal{L} = \mathcal{L}_0 \cup \mathcal{L}_1$, where $\mathcal{L}_1$ and $\mathcal{L}_0$ are the index sets of lines that meet and do not meet the conditions in (22), respectively. Without loss of generality, the lines can be re-labeled so that $\mathcal{L}_0$ corresponds to the left columns of $\boldsymbol{\Psi}$ and $\mathcal{L}_1$ to the right columns of $\boldsymbol{\Psi}$. If line $\ell \in \mathcal{L}_0$, then $\forall t \in \mathcal{K}$,

$$\sum_{i\in\mathcal{N}_\ell} \zeta_\ell p_i[t] + q_i[t] = 0. \tag{25}$$

Note that the $i^{\text{th}}$ entry in $\boldsymbol{\pi}_\ell$ is 1 if and only if bus $i$ is a downstream bus of line $\ell$. Essentially, the non-zero entries in $\boldsymbol{\pi}_\ell$, which are ones, indicate the downstream buses of line $\ell$. Therefore, it follows from (25) that, $\forall t \in \mathcal{K}$:

$$\boldsymbol{\pi}_\ell^\top \boldsymbol{\rho}_\ell[t] = 0. \tag{26}$$

Consequently, all entries in the $\ell^{\text{th}}$ column of $\boldsymbol{\Psi}[k]$ are zero, and the value of $x_\ell$ does not affect the objective function in

(11). Under such condition, $x_\ell$ cannot be identified. For line $\ell \in \mathcal{L}_0$, we can remove the $\ell^{\text{th}}$ column of $\mathbf{\Psi}[k]$, the $\ell^{\text{th}}$ entry of $\boldsymbol{x}$ and $\boldsymbol{\psi}[k]$ to obtain a reduced-size estimation problem.

Next we show that the line parameter can be identified as long as condition (22) is satisfied. Without loss of generality, we assume $\mathcal{L}_1 = \mathcal{L}$ since otherwise we can remove the left columns in $\mathbf{\Psi}$ that correspond to $\mathcal{L}_0$ to obtain a reduced problem. Then, (26) is satisfied for all $\ell \in \mathcal{L}$ and for some $t \in \mathcal{K}$. Assume $\text{rank}(\mathbf{\Psi}[k]) < L$, then there exist $a_1, \cdots, a_L \in \mathbb{R}$, which are not all zero, such that

$$\mathbf{\Psi}[k][a_1, \cdots, a_L]^\top = \mathbf{0}_{mL}, \tag{27}$$

where $\mathbf{0}_{mL}$ is an $mL$-dimensional all-zeros vector. Without loss of generality, assume $a_1, \cdots, a_{L'}$ are not zero, while $a_{L'+1}, \cdots, a_L$ are all zero, where $1 < L' \leq L$. Then, it follows from (24) and (27) that

$$\sum_{l=1}^{L'} a_l \boldsymbol{\pi}_l^\top \boldsymbol{\rho}_l[t] \boldsymbol{\pi}_l = \mathbf{0}_L. \tag{28}$$

Since $\boldsymbol{\pi}_1, \cdots, \boldsymbol{\pi}_{L'}$ are linear independent, then $a_l \boldsymbol{\pi}_l^\top \boldsymbol{\rho}_l[t] = 0$ for $\ell = 1, \cdots, L'$. However, since for any $\ell \in \mathcal{L}$ there exists some $t \in \mathcal{K}$ such that $\boldsymbol{\pi}_\ell^\top \boldsymbol{\rho}_\ell[t] = 0$, then $a_\ell = 0$ for $\ell = 1, \cdots, L'$, which leads to a contradiction. Therefore, $\text{rank}(\mathbf{\Psi}[k]) = L$ and the line parameters can be identified. □

*Remark* 2. The voltage sensitivity matrices can be readily computed if all line parameters can be identified. If some line parameter cannot be identified, the resulting voltage sensitivity matrices may not be accurate. This, however, will not have any impact on the approximate relation between voltage magnitudes and the active and reactive power injections in (20a) since in such cases the line parameter does not affect the voltage magnitudes anyway. Specifically, if follows from (1), (7), and (8) that

$$\tilde{\boldsymbol{v}}[t] = \boldsymbol{R}\boldsymbol{p}[t] + \boldsymbol{X}\boldsymbol{q}[t] = 2\sum_{\ell=1}^{L} \boldsymbol{\pi}_\ell \boldsymbol{\pi}_\ell^\top \boldsymbol{\rho}[t] x_\ell, \tag{29}$$

in which $\boldsymbol{\pi}_\ell^\top \boldsymbol{\rho}[t] = 0$ if $x_\ell$ cannot be identified. Therefore, for the purpose of solving the voltage control problem, the proposed voltage sensitivity estimation algorithm is still effective. Indeed, the parameter estimation algorithm does not really depend on the load levels in the power distribution system.

If we think of $\zeta_\ell p_i[t] + q_i[t]$ as some "combined power" (in the sense that it is a combination of active and reactive power), then (22) essentially indicates that the sum of combined power injection at all downstream buses of line $\ell$ is nonzero, or equivalently, there exists some combined power flow on line $\ell$. For any line for which the receiving end is a leaf, its parameter can be identified as long as the combined power injection at the receiving end is nonzero.

## V. Numerical Simulations

In this section, we validate the effectiveness of the proposed framework using a modified three-phase balanced IEEE 123-bus distribution test feeder from [23], the topology of which is shown in Fig. 2. There are six switches, four of which

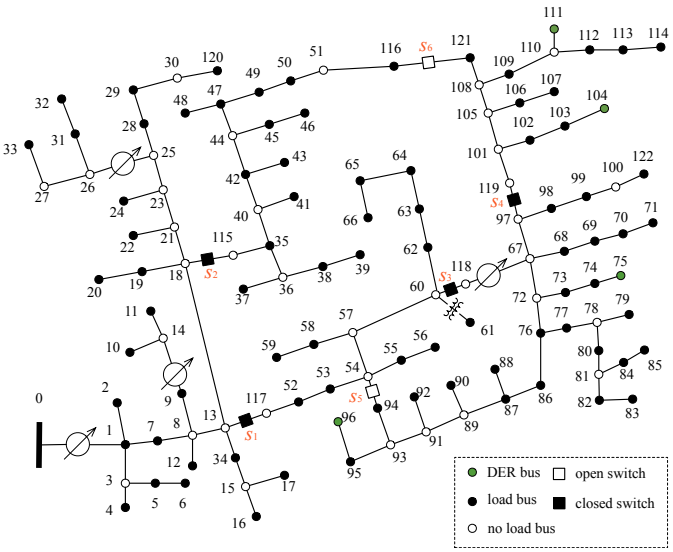


Fig. 2. IEEE 123-bus distribution test feeder. (The switch positions correspond to those of the nominal system configuration.)

TABLE I
Switch Status Under Feasible Topology Configurations.

| config. | $s_1$ | $s_2$ | $s_3$ | $s_4$ | $s_5$ | $s_6$ |
|---|---|---|---|---|---|---|
| 0 | closed | closed | closed | closed | open | open |
| 1 | closed | closed | open | closed | closed | open |
| 2 | closed | closed | closed | open | open | closed |
| 3 | closed | closed | open | closed | open | closed |
| 4 | closed | open | closed | closed | open | closed |
| 5 | open | closed | closed | closed | open | closed |
| 6 | closed | closed | open | open | closed | closed |
| 7 | closed | open | open | closed | closed | closed |
| 8 | open | closed | open | closed | closed | closed |

are normally closed while the other two are open so as to ensure the system maintains a radial topology at all times. Under Assumption **A2**, this feeder has nine possible topology configurations as listed in Table I, among which configuration 0 is the nominal one.

The loads are constructed based on historical hourly active power load data from a residential building in San Diego [24]. Specifically, the historical hourly active power load data are first normalized such that the maximum active load becomes 1. Then, the time granularity of the normalized active power load is increased to 1 second through a linear interpolation. Let $d[k]$ denote the $k^{\text{th}}$ value in the normalized 1-second active power load time series. Each value in the resulting normalized 1-second system total active power load data time series is further multiplied by a normally distributed variable, the mean and standard deviation of which is 1 and 0.01, respectively. Then, the active and reactive power demanded by load $i$ is constructed as follows:

$$p_i^d[k] = p_i^{d0} d[k](1 + 0.01\mu^p[k]),$$
$$q_i^d[k] = q_i^{d0} d[k](1 + 0.01\mu^q[k]),$$

where $p_i^{d0}$ and $q_i^{d0}$ are the nominal active and reactive power demanded by load $i$, $\mu^p$ and $\mu^q$ are two standard Gaussian random variables.

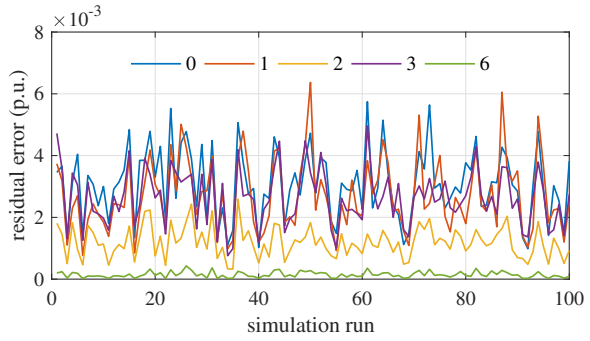


Fig. 3. Residual errors under different topology configurations with 10 sets of noise-free measurements. (Legends indicate topology configurations.)

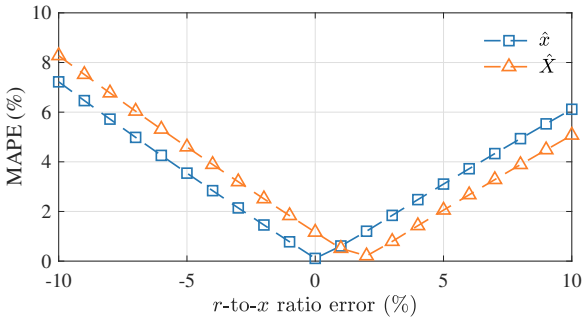


Fig. 4. Impacts of errors in $r$-to-$x$ ratios on parameter estimation accuracy in the noise-free case.

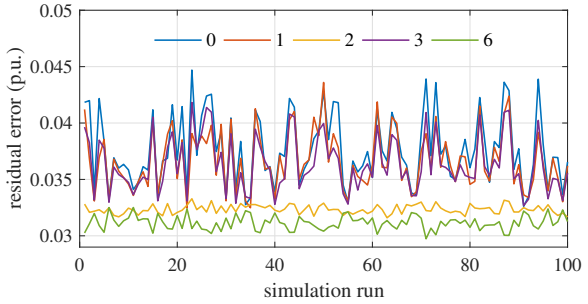


Fig. 5. Residual errors under different topology configurations with 60 sets of noisy measurements. (Noise follows Gaussian distribution. Legends indicate topology configurations.)

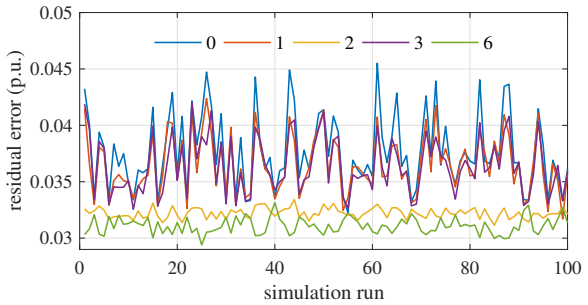


Fig. 6. Residual errors under different topology configurations with 60 sets of noisy measurements. (Noise follows Laplace distribution. Legends indicate topology configurations.)

Four DERs are added at buses 76, 97, 105, 112, respectively, with reactive power outputs taking values in the interval $[-200, 200]$ kVAr. We set the weights in (21) to $w_i^p = 1+0.1i$ and $w_i^q = 1 + 0.1i$, for $i \in \mathcal{N}^g$. For simplicity, the active power outputs from DERs are fixed at zero; yet, the proposed methodology can be directly applied to cases in which the active power outputs from DERs are nonzero. The minimum and maximum voltage magnitudes are 0.95 p.u. and 1.05 p.u., respectively. In addition, in (21), we set $\beta_1 = \beta_2 = 1 \times 10^5$. Unless otherwise specified, the forgetting factor $\eta$ in (21) is set to 1, and the underlying topology configuration is configuration 0, i.e., the nominal one. While the LinDistFlow model was adopted for the analysis and design of the estimation algorithms presented earlier, in the simulations, we use a full nonlinear power flow model and solve it using Matpower [25].

### A. Estimation Accuracy

Throughout this part, the DERs do not inject any reactive power into the power distribution system.

*1) Noise-free case:* We first evaluate the accuracy of the proposed estimation algorithm in the case where the measurements are noise-free. The algorithm is evaluated in 100 Monte Carlo simulation runs under various loading conditions. In each simulation run, 10 sets of measurements are used to compute the residual error. Residual errors are computed for each feasible topology configuration in $\mathcal{M}$, while the underlying true topology configuration is one of them. Residual errors associated with topology configurations $0-3$ and 6, when the underlying topology configuration is configuration 6, are shown in Fig. 3. Residual errors associated with topology configurations $4, 5, 7, 8$ are at least one order of magnitude larger than those of the other configurations, and are hence not plotted. Note that the case with the underlying topology configuration being configuration 6 is the one where the residual error differences between topology configurations are the smallest. Yet, it is obvious that the true topology configuration results in the minimum residual error, which is one order of magnitude smaller than those of other configurations.

The parameter estimation accuracy is evaluated using the mean absolute percentage error (MAPE), given by $\frac{1}{L}\sum_{\ell=1}^{L}|\hat{x}_\ell/x_\ell - 1|$ for $\hat{\boldsymbol{x}}$, and given by $\frac{1}{L^2}\sum_{i=1}^{L}\sum_{j=1}^{L}|\hat{X}_{ij}/X_{ij} - 1|$ for $\hat{\boldsymbol{X}}$. When one set of measurements is utilized, a typical MAPE is $0.11\%$ for $\hat{\boldsymbol{x}}$ and $1.16\%$ for $\hat{\boldsymbol{X}}$, both of which are really small. We note that the loading conditions of the power distribution system do not affect the accuracy of the proposed algorithm. The $r$-to-$x$ ratios of all lines are assumed to be known. Figure 4 shows that the MAPE is almost linear with respect to the $r$-to-$x$ ratio errors. Therefore, relatively small error in the $r$-to-$x$ ratios will not result in a significant increase in the parameter estimator error.

*2) Noisy case:* To see the impacts of measurement noise, we add a white Gaussian noise to all measurements such that the signal-to-noise ratio (SNR) is 92 dB, as adopted in [26]. More measurements across time are required to obtain a good estimation accuracy in the presence of measurement noise. The algorithm is again evaluated in 100 Monte Carlo runs under the same setup as the noise-free case, except that 60 sets of measurements—corresponding to measurements collected in 1 minute—are used to compute the residual

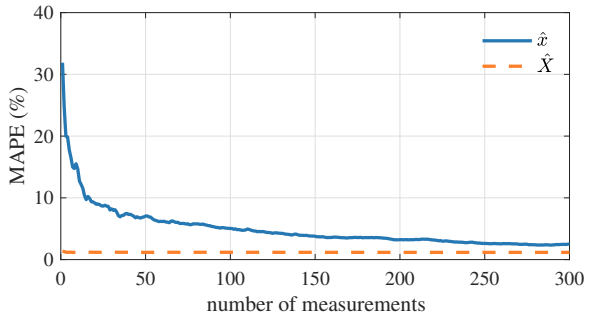


Fig. 7. Impacts of measurement numbers on parameter estimation accuracy in the noisy case.

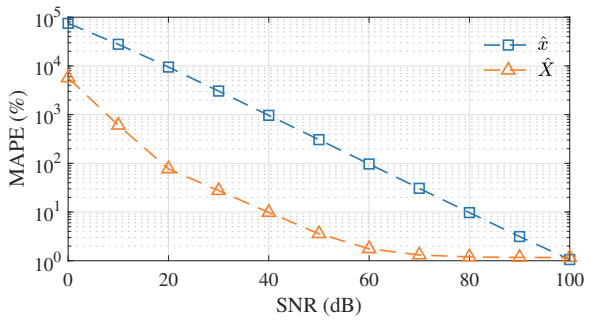


Fig. 8. Impacts of SNR on parameter estimation accuracy when 300 sets of measurements are used.

error. Residual errors associated with topology configurations $0-3$ and $6$ are shown in Fig. 5. Note that residual errors associated with topology configurations $4, 5, 7, 8$ are one order magnitude larger than those of the other configurations, and are hence not plotted. The true topology configuration, i.e., configuration $6$, still results in the minimum residual error. We note that increasing the number of measurements across time generally leads to a higher accuracy in identifying the topology configuration.

In addition to the Gaussian measurement noise, we also test our algorithm against Laplace measurement noise under the same setup. The results are quite similar to what we have observed under the Gaussian noise, as shown in Fig. 6, which shows the robustness of our algorithm against the distribution of the measurement noise.

The number of measurements has a direct impact on the estimation accuracy. As shown in Fig. 7, the MAPE of $\hat{\boldsymbol{x}}$ drops quickly when increasing the number of measurements, approximately from $31.9\%$ with one set of measurements to $2.51\%$ when 300 sets of measurements are used. The MAPE of $\hat{\boldsymbol{X}}$—which is what really matters—is relatively insensitive to the number of measurements, being around $1.17\%$. Indeed, this result illustrates the effectiveness of the proposed estimation algorithm.

Figure 8 shows the impacts of SNR on parameter estimation accuracy when 300 sets of measurements are used. When the SNR is beyond 50 dB, the MAPE of the voltage sensitivity matrix is within $3.6\%$, which is relatively small. In the rest of the simulation, we assume a SNR of 92 dB for all measurements.

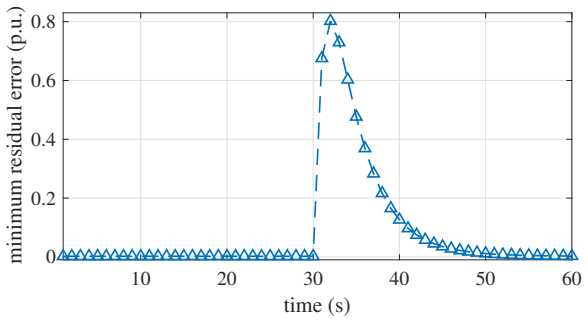


Fig. 9. Minimum residual error under topology reconfiguration.

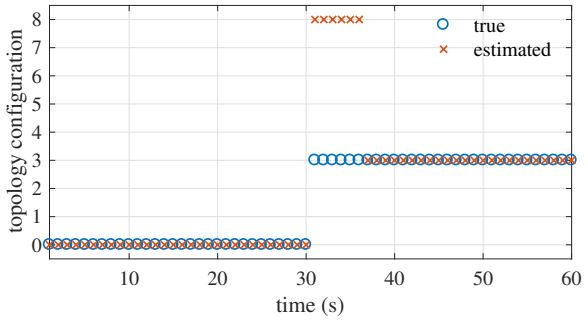


Fig. 10. Estimated topology configuration under topology reconfiguration.

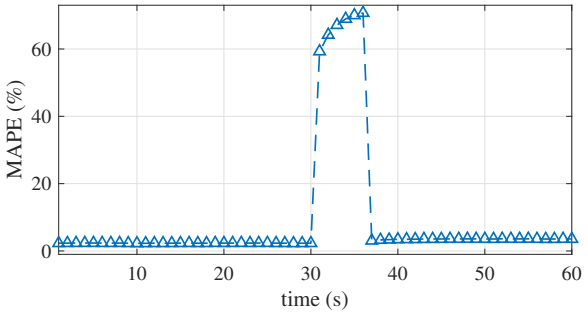


Fig. 11. MAPE of $\hat{\boldsymbol{X}}$ under topology reconfiguration.

*3) Accuracy under topology reconfiguration:* The proposed algorithm works well not only under a fixed topology configuration but also when topology reconfiguration occurs. To illustrate this, we simulate a case where the underlying topology configuration is changed from configuration $0$ to configuration $3$ at $31$ s. A total of $60$ sets of measurements are used to compute the voltage sensitivities, i.e., $|\mathcal{K}| = 60$. The forgetting factor $\eta$ is set to $0.6$. The minimum residual error and the corresponding estimated topology configuration are shown in Figs. 9 and 10, respectively. A jump in the minimum residual error is observed when the topology is reconfigured. The new topology is successfully identified after $6$ s. Correspondingly, the MAPE of $\hat{\boldsymbol{X}}$ is also reduced to less than $2\%$ after $6$ s, as shown in Fig. 11.

## B. Voltage Control Performance

Next, we show the performance of the voltage regulation framework proposed in Section III in the same case as the one in the previous section with topology reconfiguration,

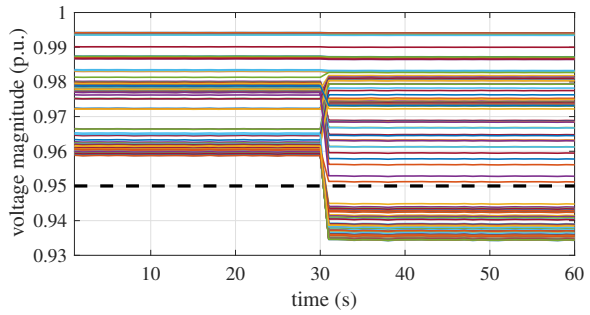


Fig. 12. Voltage profiles with model-based voltage regulation scheme under topology reconfiguration.

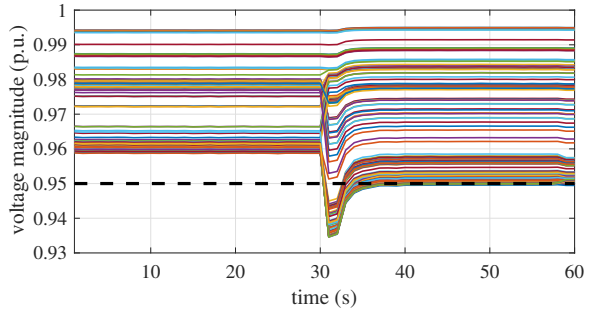


Fig. 13. Voltage profiles with proposed voltage regulation scheme under topology reconfiguration.

where the underlying topology configuration is changed from configuration 0 to configuration 3 at 31 s. A model-based voltage regulation scheme, which uses the voltage sensitivity matrices in (20a) computed from the LinDistFlow model but is not aware of the topology reconfiguration, is used for the purpose of comparison. The voltage control problem is solved using Gurobi [20]. The voltage profiles with the model-based and the proposed voltage regulation schemes are presented in Figs. 12 and 13, respectively. Since the model-based voltage regulation scheme is not aware of the topology reconfiguration, the voltage sensitivities computed from the model do not change either. As a result, the power injections from DERs remain the same, and the voltage magnitudes across the system cannot be restored. On the contrary, the voltage sensitivities estimated from the measurements will automatically adapt to the underlying changes in system conditions, and get close to the true values quickly within 6 s, as shown in Fig. 11. Consequently, the power injections from DERs will also be adjusted by the data-driven voltage regulation framework to restore the voltage magnitudes across the system to the desirable range. It is clear from these results that the proposed data-driven voltage regulation framework is effective and efficient in restoring the voltage magnitudes to the desirable range. This illustrates the adaptivity of our voltage regulation framework to system condition changes such as topology reconfiguration.

## VI. Concluding Remarks

In this paper, we proposed a data-driven voltage regulation framework for DERs in a balanced radial power distribution system. This framework utilizes a linear model that approximates the nonlinear relation between the voltage magnitudes and power injections, and estimates the voltage sensitivities indirectly by estimating the topology configuration and the corresponding line parameters. In particular, by exploiting the structural characteristics of the power distribution system, the proposed estimation algorithm for the voltage sensitivities requires much less data than existing algorithms. We also showed that the voltage sensitivities of interest are easily identifiable through a theoretical analysis.

As demonstrated in the numerical simulations, the voltage sensitivities can be accurately estimated using tens of sets of noisy measurements, which is significantly fewer than the number of measurements by existing voltage sensitivity estimation methods. In addition, the proposed voltage sensitivity estimation algorithm is robust against the types and intensity of measurement noises, as well as errors in the $r$-to-$x$ ratios. The inherent data-driven nature of the framework makes it adaptive to changes in system operational conditions, such as topology reconfigurations. This has been verified through a numerical simulation in which the voltage sensitivities can be estimated accurately using a few set of measurements even under topology reconfiguration, consequently guaranteeing good voltage regulation performance.

There are two potential directions for future work. The first is to extend the proposed framework to more complex power distribution systems that are unbalanced and may have meshed topology. A key to this extension is to develop a LinDistFlow-like model for complex power distribution systems, based on which the number of parameters in the voltage sensitivities can be reduced. The second is to develop efficient voltage sensitivity estimation algorithm for distribution systems with partial observability.

## References

[1] W. H. Kersting, *Distribution System Modeling and Analysis*. CRC press, 2006.

[2] B. A. Robbins, H. Zhu, and A. D. Domínguez-García, "Optimal tap setting of voltage regulation transformers in unbalanced distribution systems," *IEEE Transactions on Power Systems*, vol. 31, no. 1, pp. 256–267, 2015.

[3] H. Xu, A. D. Domínguez-García, and P. W. Sauer, "Optimal tap setting of voltage regulation transformers using batch reinforcement learning," *arXiv preprint arXiv:1807.10997*, 2018.

[4] B. A. Robbins, C. N. Hadjicostis, and A. D. Domínguez-García, "A two-stage distributed architecture for voltage control in power distribution systems," *IEEE Trans. Power Syst.*, vol. 28, no. 2, pp. 1470–1482, 2013.

[5] A. Kulmala, S. Repo, and P. Järventausta, "Coordinated voltage control in distribution networks including several distributed energy resources," *IEEE Transactions on Smart Grid*, vol. 5, no. 4, pp. 2010–2020, 2014.

[6] B. A. Robbins and A. D. Domínguez-García, "Optimal reactive power dispatch for voltage regulation in unbalanced distribution systems," *IEEE Trans. Power Syst.*, vol. 31, no. 4, pp. 2903–2913, 2016.

[7] B. Zhang, A. Y. Lam, A. D. Domínguez-García, and D. Tse, "An optimal and distributed method for voltage regulation in power distribution systems," *IEEE Trans. Power Syst.*, vol. 30, no. 4, pp. 1714–1726, 2015.

[8] K. Zhang, W. Shi, H. Zhu, and T. Başar, "Distributed equilibrium-learning for power network voltage control with a locally connected communication network," in *2018 Annual American Control Conference (ACC)*. IEEE, 2018, pp. 3092–3097.

[9] M. E. Baran and F. F. Wu, "Network reconfiguration in distribution systems for loss reduction and load balancing," *IEEE Trans. Power Del.*, vol. 4, no. 2, pp. 1401–1407, 1989.

[10] Y. C. Chen, A. D. Domínguez-García, and P. W. Sauer, "Measurement-based estimation of linear sensitivity distribution factors and applications," *IEEE Trans. Power Syst.*, vol. 29, no. 3, pp. 1372–1382, 2014.

[11] J. Zhang, X. Zheng, Z. Wang, L. Guan, and C. Chung, "Power system sensitivity identification–inherent system properties and data quality," *IEEE Trans. Power Syst.*, vol. 32, no. 4, pp. 2756–2766, 2017.
[12] H. Xu, A. D. Domínguez-García, and P. W. Sauer, "Adaptive coordination of distributed energy resources in lossy power distribution systems," in *2018 IEEE Power & Energy Society General Meeting (PESGM)*. IEEE, 2018, pp. 1–5.
[13] H. Xu, A. Dominguez-Garcia, and P. W. Sauer, "Data-driven coordination of distributed energy resources for active power provision," *IEEE Trans. on Power Syst.*, 2019.
[14] J. Zhang, Z. Chen, and C. He, "Identification of Var-voltage characteristics based on ambient signals," *IEEE Trans. Power Syst.*, vol. 33, no. 3, pp. 3202–3203, 2018.
[15] J. Zhang, Z. Chen, C. He, Z. Jiang, and L. Guan, "Data-driven based optimization for power system var-voltage sequential control," *IEEE Trans. Ind. Informat.*, 2018.
[16] C. Mugnier, K. Christakou, J. Jaton, M. De Vivo, M. Carpita, and M. Paolone, "Model-less/measurement-based computation of voltage sensitivities in unbalanced electrical distribution networks," in *Proc. of Power Systems Computation Conference*. IEEE, 2016, pp. 1–7.
[17] H. Zhu and H. J. Liu, "Fast local voltage control under limited reactive power: Optimality and stability analysis," *IEEE Trans. Power Syst.*, vol. 31, no. 5, pp. 3794–3803, 2015.
[18] K. Turitsyn, P. Sulc, S. Backhaus, and M. Chertkov, "Options for control of reactive power by distributed photovoltaic generators," *Proc. IEEE*, vol. 99, no. 6, pp. 1063–1073, 2011.
[19] H. Xu, A. D. Domínguez-García, and P. W. Sauer, "A data-driven voltage control framework for power distribution systems," in *2018 IEEE Power & Energy Society General Meeting (PESGM)*. IEEE, 2018, pp. 1–5.
[20] "Gurobi optimizer reference manual," Gurobi Optimization, LLC, 2019. [Online]. Available: http://www.gurobi.com
[21] D. B. West *et al.*, *Introduction to Graph Theory*. Prentice hall Upper Saddle River, 2001, vol. 2.
[22] R. B. Bapat, *Graphs and Matrices*. Springer, 2010, vol. 27.
[23] IEEE distribution test feeders. [Online]. Available: https://ewh.ieee.org/soc/pes/dsacom/testfeeders/
[24] Commercial and residential hourly load profiles for all TMY3 locations in the United States. [Online]. Available: https://openei.org/doe-opendata/dataset
[25] R. D. Zimmerman, C. E. Murillo-Sánchez, R. J. Thomas *et al.*, "MATPOWER: Steady-state operations, planning, and analysis tools for power systems research and education," *IEEE Trans. Power Syst.*, vol. 26, no. 1, pp. 12–19, 2011.
[26] L. Xie, Y. Chen, and P. R. Kumar, "Dimensionality reduction of synchrophasor data for early event detection: Linearized analysis," *IEEE Trans. Power Syst.*, vol. 29, no. 6, pp. 2784–2794, 2014.

**Hanchen Xu** received the B.Eng. and M.S. degrees in electrical engineering from Tsinghua University, Beijing, China, in 2012 and 2014, respectively, and the M.S. degree in applied mathematics and Ph.D. degree in electrical engineering from the University of Illinois at Urbana-Champaign, Urbana, IL, USA, in 2017 and 2019, respectively. His research interests include control, optimization, reinforcement learning, with applications to power systems and electricity markets.

**Alejandro D. Domínguez-García** (S'02, M'07) received the degree of electrical engineering from the University of Oviedo (Spain) in 2001 and the Ph.D. degree in electrical engineering and computer science from the Massachusetts Institute of Technology, Cambridge, MA, in 2007.

He is Professor with the Department of Electrical and Computer Engineering (ECE), and Research Professor with the Coordinated Science Laboratory and the Information Trust Institute, all at the University of Illinois at Urbana-Champaign. He is affiliated with the ECE Power and Energy Systems area, and has been a Grainger Associate since August 2011.

His research interests are in the areas of system reliability theory and control, and their applications to electric power systems, power electronics, and embedded electronic systems for safety-critical/fault-tolerant aircraft, aerospace, and automotive applications.

Dr. Domínguez-García received the NSF CAREER Award in 2010, and the Young Engineer Award from the IEEE Power and Energy Society in 2012. In 2014, he was invited by the National Academy of Engineering to attend the US Frontiers of Engineering Symposium, and was selected by the University of Illinois at Urbana-Champaign Provost to receive a Distinguished Promotion Award. In 2015, he received the U of I College of Engineering Dean's Award for Excellence in Research.

He is currently an editor for the IEEE Transactions on Control of Network Systems; he also served as an editor of the IEEE Transactions on Power Systems and IEEE Power Engineering Letters from 2011 to 2017.

**Venugopal V. Veeravalli** (M'92, SM'98, F'06) received the B.Tech. (Silver Medal Hons.) degree in electrical engineering from the Indian Institute of Technology, Bombay, India, in 1985, the M.S. degree in electrical engineering from Carnegie Mellon University, Pittsburgh, PA, USA, in 1987, and the Ph.D. degree in electrical engineering from the University of Illinois at Urbana-Champaign, Champaign, IL, USA, in 1992.

He joined the University of Illinois at Urbana-Champaign in 2000, where he is currently the Henry Magnuski Professor with the Department of Electrical and Computer Engineering, and where he is also affiliated with the Department of Statistics, the Coordinated Science Laboratory, and the Information Trust Institute. From 2003 to 2005, he was a Program Director for communications research at the U.S. National Science Foundation, Arlington, VA, USA. He has previously held academic positions at Harvard University, Rice University, and Cornell University, and has been on sabbatical at MIT, IISc Bangalore, and Qualcomm, Inc. His research interests include statistical signal processing, machine learning, detection and estimation theory, information theory, and stochastic control, with applications to sensor networks, cyberphysical systems, and wireless communications. A recent emphasis of his research has been on signal processing and machine learning for data science applications.

Prof. Veeravalli was a Distinguished Lecturer for the IEEE Signal Processing Society from 2010 to 2011. He has been on the Board of Governors of the IEEE Information Theory Society. He has been an Associate Editor for Detection and Estimation for the IEEE Transactions on Information Theory and for the IEEE Transactions on Wireless Communications. He was the recipient (for research and teaching) of the IEEE Browder J. Thompson Best Paper Award, the National Science Foundation CAREER Award, and the Presidential Early Career Award for Scientists and Engineers, and the Wald Prize in Sequential Analysis.

**Peter W. Sauer** (S'73, M'77, SM'82, F'93, LF'12) obtained his Bachelor of Science degree in electrical engineering from the University of Missouri at Rolla in 1969. From 1969 to 1973, he was the electrical engineer on a design assistance team for the Tactical Air Command at Langley Air Force Base, Virginia. He obtained the Master of Science and Ph.D. degrees in Electrical Engineering from Purdue University in 1974 and 1977 respectively. From August 1991 to August 1992 he served as the Program Director for Power Systems in the Electrical and Communication Systems Division of the National Science Foundation in Washington D.C. He is a cofounder of the Power Systems Engineering Research Center (PSERC) and the PowerWorld Corporation. He is a registered Professional Engineer in Virginia and Illinois, a Fellow of the IEEE, and a member of the U.S. National Academy of Engineering. He is currently the Grainger Chair Professor of Electrical Engineering at Illinois. Additional information can be found at: https://ece.illinois.edu/directory/profile/psauer.